

## Two scale modeling of behaviors of granular structure: size effects and displacement fluctuations of discrete particle assembly

Xihua Chu<sup>\*</sup>, Cun Yu, Chenxi Xiu and Yuanjie Xu

*Department of Engineering Mechanics, Wuhan University, Wuhan 430072, China*

*(Received October 23, 2014, Revised June 11, 2015, Accepted June 15, 2015)*

**Abstract.** This study's primary aim is to check the existence of a representative volume element for granular materials and determine the link between the properties (responses) of macro structures and the size of the discrete particle assembly used to represent a constitutive relation in a two-scale model. In our two-scale method the boundary value problem on the macro level was solved using finite element method, based on the Cosserat continuum; the macro stresses and modulus were obtained using a solution of discrete particle assemblies at certain element integration points. Meanwhile, discrete particle assemblies were solved using discrete element method under boundary conditions provided by the macro deformation. Our investigations focused largely on the size effects of the discrete particle assembly and the radius of the particle on macro properties, such as deformation stiffness, bearing capacity and the residual strength of the granular structure. According to the numerical results, we suggest fitting formulas linking the values of different macro properties (responses) and size of discrete particle assemblies. In addition, this study also concerns the configuration and displacement fluctuation of discrete particle assemblies on the micro level, accompanied with the evolution of bearing capacity and deformation on the macro level.

**Keywords:** granular materials; two-scale modeling; representative volume element; strain localization; displacement fluctuation

---

### 1. Introduction

Granular materials, such as sand and gravel, are aggregates of solid particles in contact with each other. Though they exist extensively in nature and are widely used in engineering, these materials are not well understood. Many discrete particle models and continuum models have been suggested in order to describe the complex behaviors of granular materials on the micro scale/level or on the macro scale/level (Zhou and Sun 2013, Scholtes and Donze 2013, Yu *et al.* 2013, Wan and Li 2013, Jiang *et al.* 2014, Cil and Alshibli 2014). At the macro level, these materials are typically regarded as continuum media, and a number of constitutive models have been developed to describe their behaviors in engineering analyses. However, most constitutive models are generally phenomenological, in which some parameters are vague insofar as their physical meaning is concerned. At the micro level, the discrete particle model is close to the discrete nature

---

<sup>\*</sup>Corresponding author, Associate Professor, E-mail: Chuxh@whu.edu.cn

of granular materials and can easily obtain detailed information on the particle level; however, the high computational cost constrains this model's application in real engineering analyses. The two-scale model, on the other hand, combines the advantages of continuum models and discrete particle models, providing a new approach for simulating granular materials (Christian and Peter 2012, Guo and Zhao 2014, Nitka *et al.* 2011). The framework of the two-scale model is shown in Fig. 1(a), demonstrating that the boundary value problem on the macro-level/macro scale, a continuous problem, can be solved using Finite Element Method (FEM). However, during the solution of FEM, the calculations for macro stresses and modulus tensor do not require an explicit constitutive model, resorting instead to homogenization of micro information regarding discrete particle assembly set on an integration point. The evolution of micro information regarding discrete particle assembly, including the contact forces between particles and particle positions, is driven by boundary conditions from the deformation of the corresponding integration points on the macro level.

Given the above, the key problems of the two-scale model include the question of how to impose boundary conditions on the discrete particle assembly and the homogenization of detailed micro information. Miehe (2010) considered the elliptical particle model on the micro scale and suggested a consistent extension of classical stiff, soft and periodic boundary conditions from the continuum to the particle assembly; Li *et al.* (2010), Liu *et al.* (2014) analyzed the micro-to-macro homogenization when considering the Cosserat continuum model on the macro scale based on the Hill-Mandel condition. It has been noted that the information interchange between the macro and micro levels is based on the representative volume element (RVE). Therefore all two-scale studies are based on the precondition that the RVE exists, which means there is a discrete particle assembly that can represent the macroscopic mechanical properties of granular materials. However, Gitman *et al.* (2007, 2008) found that the RVE does not exist for softening or localization, and suggested an approach implementing the coupled-volume multi-scale modeling of quasi-brittle material. Graham and Yang (2003) also doubted whether softening materials had RVE. Zhao *et al.* (2015) found the R-curve of concrete-like quasi-brittle materials is greatly dependent on specimen geometry in terms of the initial crack length. Therefore it is significant to check the existence of RVE for granular materials based on two-scale modeling, because localization and softening are important behaviors of granular materials. It has been noted that some investigations regarding the size effects of numerical specimens on macro behaviors have been carried out based on the DEM simulation (Shen 2001, Kuhn and Bagi 2009, Huang *et al.* 2013, Koyama *et al.* 2007). However, the role of specimen sizes on the response of structure may be different from that of discrete particle assemblies representing the material point. The reason for this is because the structure response is the combination of many responses from a number of material points. However, the macro strain at different integration points may be different as a result of non-uniform deformation in granular structures. Some material points are in the elastic range, while other material points are in the plastic range. This causes the diversity of boundary conditions responding to discrete particle assemblies at different integration points. It is known that the effects of size upon a discrete particle assembly representing the material points may be different according to different boundary conditions. Therefore it is more reasonable that the size effects of the specimen on the granular structure's response are investigated based on two-scale modeling. This approach reflects the resultant effects of sample size under various boundary conditions.

This study is based on the two-scale scheme, which focuses on the influence of size on the discrete particle assembly and the influence of particle radius on the ultimate bearing capacity, the

residual capacity and the macro stiffness. In this work we suggest fitting formulas to link the values of different macro physical properties and the sizes of discrete particle assemblies. Using these formulas we were able to obtain the RVE size corresponding to different macro physical properties. In addition, this study shows that the changing configurations and the particles' displacement fluctuation in the discrete particle assembly accompany the evolution of macro bearing forces and deformation.

## 2. A FEM-DEM two-scale method based on the Cosserat continuum-discrete particle model

### 2.1 Cosserat continuum and FEM on the macro level

In this two-scale model, the Cosserat continuum was adopted on the macro scale. Every material point of a two-dimensional Cosserat continuum has three independent degrees of freedom

$$\mathbf{u} = [u_x \ u_y \ \omega_z]^T, \quad (1)$$

where  $u_x$ ,  $u_y$  are the translation degrees of freedom and  $\omega_z$  is the rotation degree of freedom. The strain and stress vectors can be described as follows

$$\boldsymbol{\varepsilon} = [\varepsilon_{xx} \ \varepsilon_{yy} \ \varepsilon_{zz} \ \varepsilon_{xy} \ \varepsilon_{yx} \ \kappa_{zx} l_c \ \kappa_{zy} l_c]^T, \quad (2)$$

$$\boldsymbol{\sigma} = [\sigma_{xx} \ \sigma_{yy} \ \sigma_{zz} \ \sigma_{xy} \ \sigma_{yx} \ m_{zx}/l_c \ m_{zy}/l_c]^T, \quad (3)$$

where  $\kappa_{zx}$ ,  $\kappa_{zy}$  are the micro-curvatures and  $m_{zx}$ ,  $m_{zy}$  are the coupled stresses.  $l_c$  is the internal length scale, which is a comprehensive characterization of micro information, such as particle size and shape, relates to the width of shear bands on the macro level when the Cosserat continuum is used to describe granular materials (Muhlhaus and Vardoulakis 1987, Voyiadjis *et al.* 2005). The geometric equation of the Cosserat continuum is as follows

$$\varepsilon_{xx} = \frac{\partial u_x}{\partial x}, \quad \varepsilon_{yy} = \frac{\partial u_y}{\partial y}, \quad (4)$$

$$\varepsilon_{xy} = \frac{\partial u_y}{\partial x} - \omega_z, \quad \varepsilon_{yx} = \frac{\partial u_x}{\partial y} + \omega_z, \quad (5)$$

$$\kappa_{zx} = \frac{\partial \omega_z}{\partial x}, \quad \kappa_{zy} = \frac{\partial \omega_z}{\partial y}. \quad (6)$$

It is assumed that strain  $\boldsymbol{\varepsilon}$  can decompose into the elastic strain  $\boldsymbol{\varepsilon}_e$  and the plastic strain  $\boldsymbol{\varepsilon}_p$ , and the elastic strain is supposed to satisfy the linear stress-strain relationship

$$\boldsymbol{\sigma} = \mathbf{D}_e \boldsymbol{\varepsilon}_e, \quad \boldsymbol{\varepsilon}_e = [\mathbf{D}_e]^{-1} \boldsymbol{\sigma}, \quad (7)$$

$$\mathbf{D}_e = \begin{bmatrix} \lambda+2G & \lambda & \lambda & 0 & 0 & 0 & 0 \\ \lambda & \lambda+2G & \lambda & 0 & 0 & 0 & 0 \\ \lambda & \lambda & \lambda+2G & 0 & 0 & 0 & 0 \\ 0 & 0 & 0 & G+G_c & G-G_c & 0 & 0 \\ 0 & 0 & 0 & G-G_c & G+G_c & 0 & 0 \\ 0 & 0 & 0 & 0 & 0 & 2G & 0 \\ 0 & 0 & 0 & 0 & 0 & 0 & 2G \end{bmatrix}, \quad (8)$$

where  $G$  and  $\nu$  are the shear modulus and the Poisson ratio in the classical continuum model, respectively,  $\lambda=2G\nu/(1-2\nu)$ , while  $G_c$  is the Cosserat shear modulus.

The static equilibrium equation for the Cosserat continuum model under a two-dimensional case is composed using 3 equations

$$\begin{cases} \frac{\partial \sigma_{xx}}{\partial x} + \frac{\partial \sigma_{yx}}{\partial y} + F_x = 0 \\ \frac{\partial \sigma_{xy}}{\partial x} + \frac{\partial \sigma_{yy}}{\partial y} + F_y = 0 \end{cases}, \quad (9)$$

$$\frac{\partial m_{zx}}{\partial x} + \frac{\partial m_{zy}}{\partial y} - (\sigma_{yx} - \sigma_{xy}) + M_z = 0, \quad (10)$$

where  $F_x$ ,  $F_y$ ,  $M_z$  are the body forces and torque in the corresponding directions.

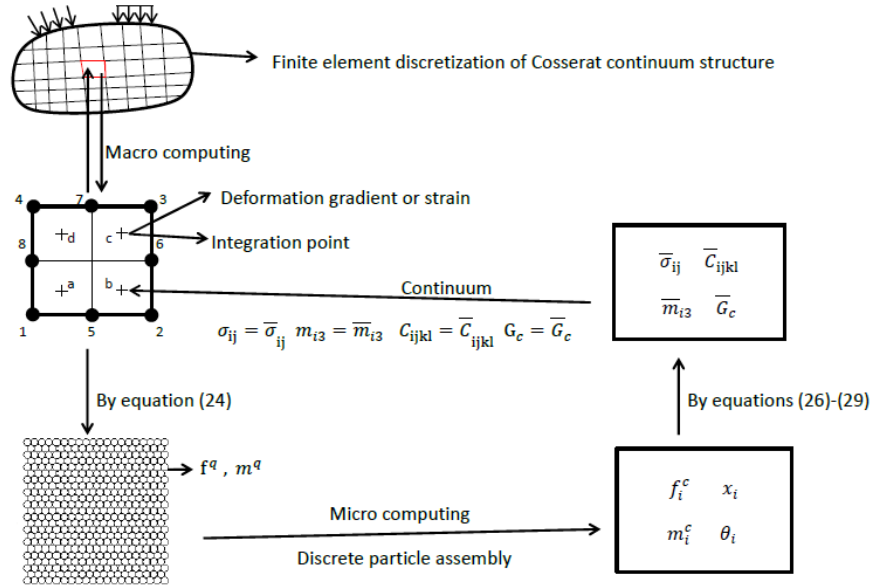
Introduced in the Cosserat continuum are: a rotational degree of freedom with the rotation axis orthogonal to the 2D plane, micro-curvatures as spatial derivatives of the rotational degree of freedom, couple stresses conjugated to the micro-curvatures and the material parameter defined as internal length scale. The boundary value problem based on the Cosserat continuum is solved using FEM. For the each incremental step on the macro scale, the macro deformation will be transformed into boundary conditions of discrete particle assemblies at the elements' integration points in order to drive the computation on the micro level. According to the computational results, the macro stresses and deformation modulus tensor are obtained. This study adopted an eight-node plane rectangular element with reduced integration, which means that each element has four Gauss integral points. The discrete particle assembly is assigned to each integral point, as shown in Fig. 1.

## 2.2 Discrete particle model and DEM on the micro level

In this two-scale model, a discrete particle model in which the granular materials are regarded as an assembly with discrete particles in contact with each other, has been adopted on the micro level. The assembly's solutions are provided by DEM, the main ideas of which include two folds: the first is the calculation of contact forces between particles, and the other is the solution for the particle motion equation.

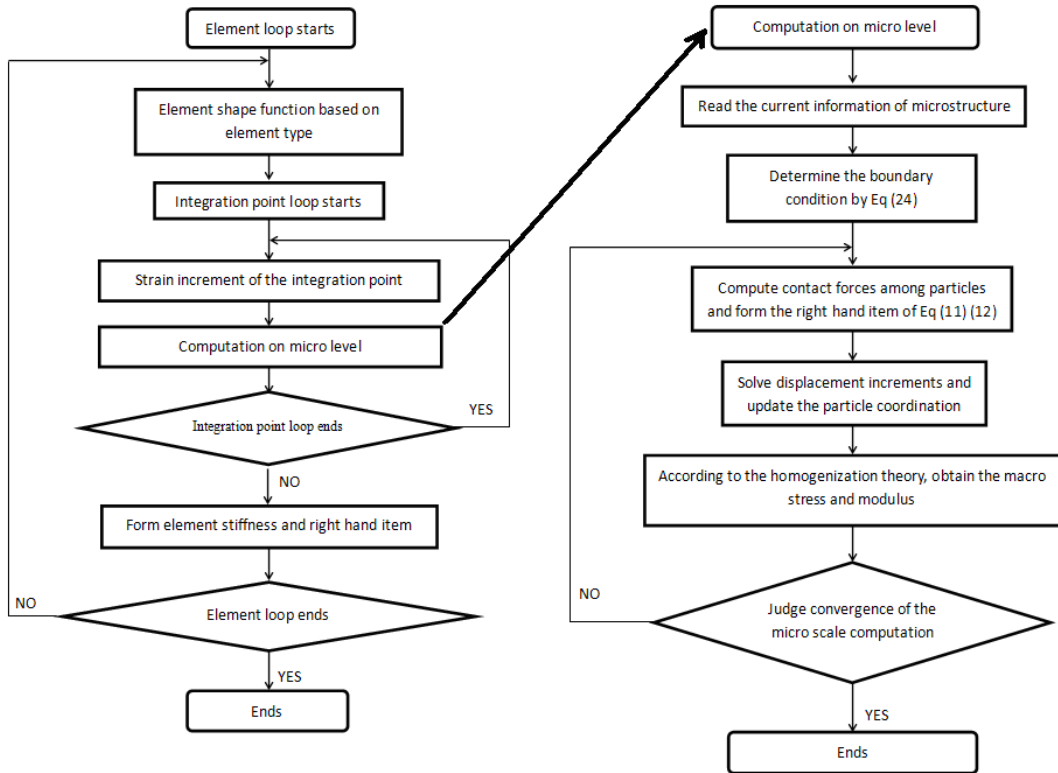
For a typical particle  $a$ , the following equations of motion in the two-dimensional case are given

$$m_a \frac{d\mathbf{v}_a}{dt} = \sum_{j=1}^{k_a} \mathbf{f}^{cj} + m_a \mathbf{g} + \mathbf{f}^e, \quad (11)$$



Note: black round points represent 8 nodes of an element, cross points represent 4 Gauss integration points.

(a)



(b)

(c)

Fig. 1 The diagram and flow chart of computational two-scale modeling: (a) the diagram (b) the flow chart for computation on an element (c) the flow chart for computation on the micro level

$$I_a \frac{d\omega_a}{dt} = \sum_{j=1}^{k_a} (\mathbf{r}_a^j \times \mathbf{f}^{cj} + M_r^j), \quad (12)$$

Where  $m_a$  and  $I_a$  are, respectively, the mass and the mass moment of inertia of particle  $a$ .  $\mathbf{v}_a$  and  $\omega_a$  stand for, respectively, the translational velocity vector and the angular velocity of particle  $a$ ,  $k_a$  is the number of particles in contact with particle  $a$ ,  $\mathbf{f}^{cj}$  is the contacting force vector exerted by a neighboring particle  $j$  on particle  $a$ ,  $\mathbf{g}$  is the gravity acceleration vector,  $\mathbf{f}^e$  is the other external force vector,  $\mathbf{r}_a^j$  is the vector from the center of particle  $a$  to its contact point with particle  $j$ , and  $M_r^j$  is the rolling friction resistance moment exerted by particle  $j$  on particle  $a$ . In this study, we used an explicit integration algorithm to solve equations of motion.

The contacting forces between particles are calculated as follows. As the incremental step  $I_n=[t_n, t_{n+1}]$  is considered, the normal contact force is related to the relative normal movement measurement i.e., the ‘‘overlap’’  $u_N^{j,n+1}$  at the current time instant  $t_{n+1}$  and its variation rate with respect to time.  $u_N^{j,n+1}$  is defined as the difference between the sum of the two particles’ radii and the distance between the centers of the two particles, i.e.

$$u_N^{j,n+1} = r_a + r_j - \|\mathbf{X}(A_o^{n+1}) - \mathbf{X}(B_o^{j,n+1})\|, \quad (13)$$

where  $r_a, \mathbf{X}(A_o^{n+1}), r_j, \mathbf{X}(B_o^{j,n+1})$  are the radius and the coordinates of the centers of particles  $a$  and  $j$ , respectively. The normal contact force  $F_N^j$  between the two particles  $a$  and  $j$  can be calculated by

$$F_N^j = -k_N u_N^{j,n+1} - c_N \frac{u_N^{j,n+1} - u_N^{j,n}}{\Delta t} \quad \text{if } u_N^{j,n+1} > 0, \quad (14)$$

$$F_N^j = 0 \quad \text{if } u_N^{j,n+1} \leq 0, \quad (15)$$

where  $k_N$  and  $c_N$  are the compression stiffness coefficient and the coefficient of viscous damping of the normal contact deformation for granular materials.

The predictor  $F_{s,tr}^{j,n+1}$  of the tangential friction force at  $t_{n+1}$  due to relative tangential sliding,  $\Delta u_s^j$  can be estimated as

$$F_{s,tr}^{j,n+1} = f_s^{j,n+1} + d_s^{j,n+1}, \quad (16)$$

in which

$$f_s^{j,n+1} = f_s^{j,n} + \Delta f_s^j; \quad \Delta f_s^j = -k_s \Delta u_s^j; \quad d_s^{j,n+1} = -c_s \frac{du_s^j}{dt}, \quad (17)$$

where  $k_s, c_s$  stand for the stiffness coefficient and the coefficient of viscous damping of sliding tangential friction.  $F_{s,tr}^{j,n+1}$  has to satisfy the Coulomb law of friction, and the rolling/sliding friction tangent force is determined by

$$F_s^j = F_{s,tr}^{j,n+1} \quad \text{if } |F_{s,tr}^{j,n+1}| \leq \mu_s |F_N^{j,n+1}|, \quad (18)$$

$$F_s^j = \text{sign}(F_{s,tr}^{j,n+1}) \mu_s |F_N^{j,n+1}| \quad \text{if } |F_{s,tr}^{j,n+1}| > \mu_s |F_N^{j,n+1}|, \quad (19)$$

where  $\mu_s$  is the (maximum) static sliding tangential friction coefficient.

To calculate  $M_r^j$  at  $t_{n+1}$ , we first have to estimate its predictor  $M_{r,tr}^{j,n+1}$  due to the relative rolling angular displacement increment  $\Delta\theta_r^j (d\theta_r^j)$

$$M_{r,tr}^{j,n+1} = M_{rs}^{j,n+1} + M_{rv}^{j,n+1} , \quad (20)$$

in which

$$M_{rs}^{j,n+1} = M_{rs}^{j,n} + \Delta M_{rs}^j ; \quad \Delta M_{rs}^j = -k_r \Delta\theta_r^j ; \quad M_{rv}^{j,n+1} = -c_r \frac{d\theta_r^j}{dt} , \quad (21)$$

where  $k_r$  and  $c_r$  stand for the stiffness coefficient and the coefficient of viscous damping of the rolling friction moment, respectively.  $M_{r,tr}^{j,n+1}$  has to satisfy the Coulomb law of friction; the rolling friction resistance moment is then determined by

$$M_r^j = M_{r,tr}^{j,n+1} \quad \text{if} \quad |M_{r,tr}^{j,n+1}| \leq \mu_\theta r |F_N^j| , \quad (22)$$

$$M_r^j = \text{sign}(M_{r,tr}^{j,n+1}) \mu_r r |F_N^j| \quad \text{if} \quad |M_{r,tr}^{j,n+1}| > \mu_r r |F_N^j| , \quad (23)$$

where  $\mu_r$  and  $r$  are the (maximum) static rolling friction moment coefficient and the radius of the particle in consideration, respectively.

### 2.3 Macro-to-micro connection

The key component of the two-scale method is the exchange of information between the macro scale and micro scale, which is usually implemented based on the concept of RVE. RVE is a large enough sample of the material that allows it to be used to determine the corresponding macro effective properties through the homogenization of micro information. The RVE boundary conditions are obtained from the transformation of the macro displacement gradient, which needs to be consistent with the Hill-Mandel type condition (Hill 1985, Liu *et al.* 2014). This study has adopted a penalty-type implementation of boundary constraints outlined first by Miehe (2010)

$$\mathbf{f}_q = -\frac{\varepsilon_f}{V} (\mathbf{x}_q - \bar{\mathbf{F}} \mathbf{X}_q) \quad \mathbf{m}_q = -\frac{\varepsilon_c}{V} (\mathbf{q}_q - \mathbf{1}) , \quad (24)$$

where subscript  $q$  expresses  $q$  th particle on the boundary of the particle assembly,  $V$  is the size of the discrete particle assembly at the micro scale (it stands for the area under 2D case),  $\mathbf{f}_q$ ,  $\mathbf{m}_q$  are, respectively, the support force and the support couple at  $q$  th particle,  $\mathbf{x}_q$ ,  $\mathbf{q}_q$  are the current coordinates and the rotation angle of  $q$  th particle's centroid,  $\mathbf{X}_q$  is the original coordinate.  $\varepsilon_f$  and  $\varepsilon_c$  are the computational parameters.

The purpose of this study is to investigate the influence of a discrete assembly's size on the micro level in two-scale modeling. Therefore, strictly speaking, the discrete assembly used in this study cannot be referred to as RVE if the size of the discrete particle assembly (SDPA) has an effect on macro properties. At present, most two-scale modeling predicts macro properties based on such discrete assemblies at the micro level; however, it must be clear that this RVE is only the numerical sample used to average micro information.

Based on homogenization, the macro stress and deformation modulus can be obtained as

follows. Considering that the shear forces at a contact are not coupled with the normal displacement, the contact stiffness  $k_{ij}$  can be written as

$$k_{ij} = k_n n_i n_j + k_s s_i s_j, \quad (25)$$

Where  $n_i, s_i$  are the respective components of the unit contact normal vector and tangential vector. The deformation modulus tensor  $C$  and the mean stress of the packing  $\bar{\sigma}$  can be expressed in terms of components as

$$C_{ijkl} = \frac{1}{2V} \sum_n \sum_p l_i^{np} k_{jl}^{np} l_k^{np}, \quad (26)$$

$$\bar{\sigma}_{ij} = \frac{1}{2V} \sum_{n=1}^N \sum_{\substack{p=1 \\ p \neq n}}^N f_i^{np} l_j^{np}, \quad (27)$$

Where  $k_{ji}^{np}$  is the contact stiffness between particles  $n$  and  $p$ ,  $l_j^{np}$  is the branch vector joining the centroids of particles  $n$  and  $p$  in contact,  $f_i^{np}$  is the contact force vector between particles  $n$  and  $p$ . Meanwhile, the rotation modulus  $\bar{G}_c$  and the mean couple of the packing  $\bar{m}_{13}$  and  $\bar{m}_{23}$  can be expressed as

$$\bar{m}_{i3} = \frac{1}{2V} \sum_{n=1}^N \sum_{\substack{p=1 \\ p \neq n}}^N M^{np} l_i^{np}, \quad (28)$$

$$\bar{G}_c = \frac{2N_c r^2}{V} k_r, \quad (29)$$

where  $N_c$  is the total number of contacts in the particle assembly. Here, the mean stress  $\bar{\sigma}_{ij}$  and the mean couple  $\bar{m}_{13}$  and  $\bar{m}_{23}$  are regarded as the stress and couple stress of the Cosserat continuum on the macro level. The deformation modulus tensor and the rotation modulus, which came from the discrete assembly, will serve as the modulus tensor on the macro level.

In conclusion, the two-scale procedure for granular materials based on a discrete particle model (on the micro level) and the Cosserat continuum (on the macro level) is similar to the procedure for heterogeneous materials or complex materials (Gitman *et al.* 2008). All of these procedures contain a downscaling and upscaling process. During the downscaling process the deformation information on the macro level is converted as the boundary conditions of the discrete particle assembly at the micro level. In this study, the penalty-type boundary constraints, Eq. (24), were implemented on the discrete assembly at the micro level. Driven by the boundary conditions, the discrete assembly solution was solved using DEM, and the corresponding information, such as contact forces and contact norm vectors, were obtained. The upscaling was then carried out through Eqs. (26)-(29) to obtain the macro stress and deformation modulus. This macro stress and deformation modulus will serve for the solution of the displacement of the Cosserat continuum on the macro level. The diagram and flow chart of computational two-scale modeling is presented in Fig. 1.

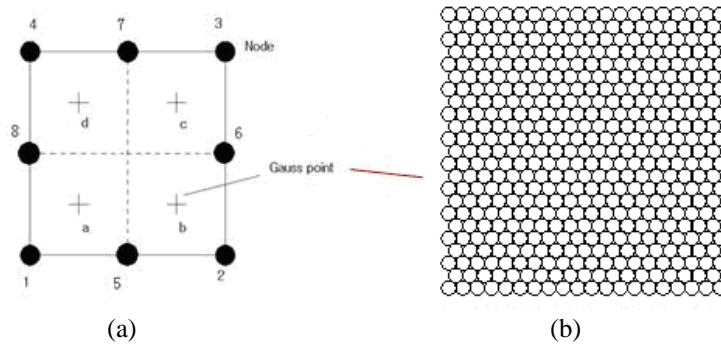


Fig. 2 Sketch of element: (a) Eight black points stand for nodes of element and four cross points stand for Gauss integral points; (b) The particle assembly at the Gauss integral point

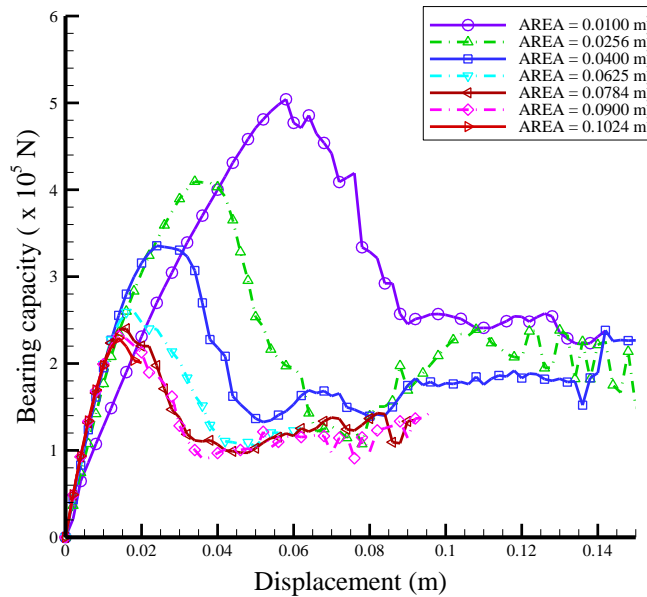


Fig. 3 Curves of the bearing capacity vs. the vertical displacement

### 3. The size of the discrete particle assembly

The discrete particle assembly is the physical basis of information transformation between the macro and micro scale. The size of the discrete particle assembly has a significant effect on macro properties determined through discrete element simulation (Koyama and Jing 2007, Kuhn and Bagi 2009, Huang *et al.* 2014). In this section, the influences of the discrete particle assembly size on the ultimate bearing capacity, the residual capacity and the macro stiffness of granular material structure are investigated based on two-scale modeling.

On the macro scale, a homogeneous 1×1 m<sup>2</sup> square panel is considered. The vertical load is applied to the top and bottom of the panel with increasing prescribed vertical displacement. This panel is meshed into four 8-node quadrilateral reduced integration elements (as shown in Fig. 2(a)). Each element has four integration points, and assigned on each integration point are discrete

particle assemblies, consisting of 5 mm round particles with a dense arrangement (as shown in Fig. 2(b)). The micro parameters used in the simulation are as follows:

$k_n=6.7\times 10^7$  N/m,  $k_s=3.4\times 10^7$  N/m,  $k_r=25$  N·m/rad,  $\mu_s=0.5$ ,  $\mu_r=0.2$ ,  $c_s=0$ ,  $c_r=0$ . The computational parameters  $\varepsilon_f=6.7\times 10^6$ ,  $\varepsilon_c=1.0\times 10^3$ .

In this scheme of two-scale modeling, computations on the macro level using FEM are considered convergence if one force criterion or one displacement criterion are satisfied, while computation on the micro level using DEM is considered as convergence when the total kinetic energy of the discrete particle assembly is less than the tolerance; this is the convergence criterion commonly used to solve for the discrete element method using the dynamic relax algorithm.

The total reaction of the nodes on the top boundary, which is referred to as the capacity or the load of the macro structure, varies with vertical displacement. Given the discrete particle assembly on the micro level, the maximum capacity is denoted as the structure's bearing capacity on the macro level during the displacement loading. On the load-displacement diagram, the bearing capacity can be obtained according to the peak of curve of load-displacement. For the load-displacement curve of the geo-structure, the load present the minimum value remains approximately constant after the peak as a result of softening, which is referred to as residual capacity in this study. Fig. 3 shows load-vertical displacement curves under various sizes of discrete particle assemblies. It can be observed that the slopes of these curves almost coincide with the linear elastic regime (before displacement of 0.01 m), excluding the curve corresponding to the sample with a volume of 0.01 m<sup>2</sup>. We have denoted the ratio of load and the displacement of the structure as the macro stiffness; this means that the macro stiffness has RVE in the elastic range. The bearing capacity and residual capacity decreases as the sample volume increases until the volume increases to critical value. This indicates they have also RVE; however, the RVE size of the bearing capacity is not identical to that of the residual capacity. In this study, the size of the RVE for the bearing capacity may take more than 0.0784 m<sup>2</sup>, while that of the residual capacity may take more than 0.0625 m<sup>2</sup>. This also means the RVE of the bearing capacity is greater than that of the residual capacity. In order to better show the evolution of macro-properties, such as macro stiffness, bearing capacity and residual capacity with the size of the discrete particle assembly, the data from Fig. 3 have been re-plotted as shown in Fig. 4. It is important to note that in Fig. 5 the macro stiffness is defined as the ratio of half the bearing capacity and the corresponding vertical displacement, which includes the effects of plasticity. From Fig. 4 we see that the macro stiffness increases with the increasing size of the discrete particle assembly to approach a limit value. This means that RVE does exist for the macro stiffness. However, in this study, the macro stiffness increases with the SDPA. This tendency may be contributed to the boundary condition provided by Eq. (24), which is similar to a membrane condition or a flexible boundary. It has been noted that when the rigid boundary was used, the discrete simulation indicates that the stiffness decreased with an increasing sample size (Koyama and Jing 2007). In fact, in Fig. 3 we can see that all the curves nearly coincide before peaking beside the curve corresponding to the size of the discrete particle assembly 0.01 m<sup>2</sup>. This is the reason discrete particle assemblies with sizes under 0.01 m<sup>2</sup>, only containing 90 particles, are too small to represent macro physical quantities.

It can be deduced from Fig. 4 that the RVE also exists for the ultimate bearing capacity and the residual strength. As shown in Fig. 4, the ultimate bearing capacity and the residual strength decrease as the size of the particle assembly increases until they approach corresponding critical representative values for a large enough discrete particle assembly. However, the size of the RVE responding to the macro stiffness, as well as the ultimate bearing capacity and the residual strength

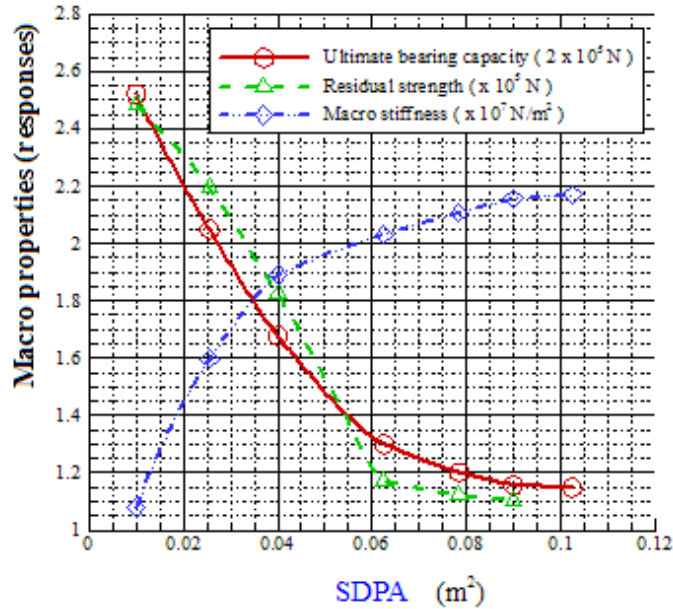


Fig. 4 Curves of area of the assembly vs. ultimate bearing capacity, residual strength and structural stiffness

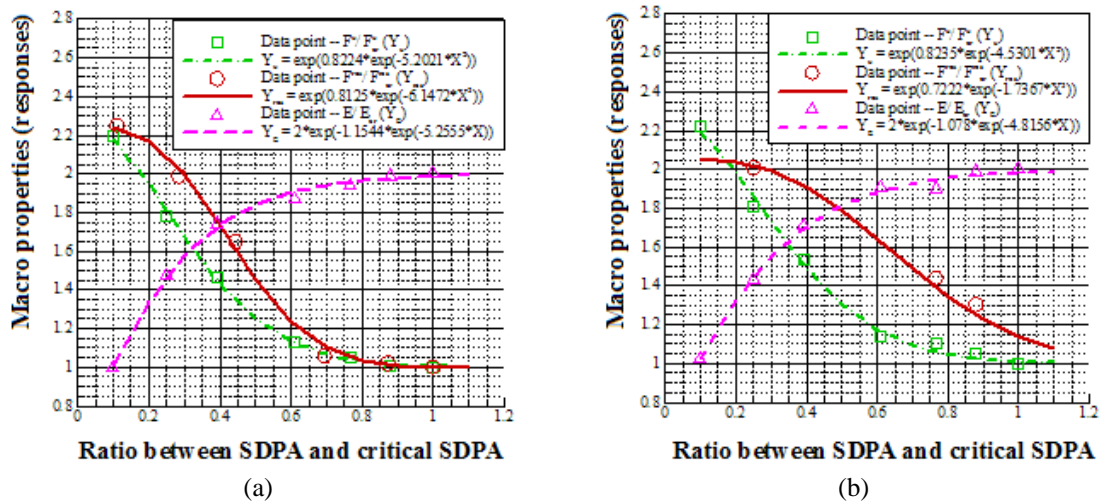


Fig. 5 Data fit curve of the area of the assembly vs. ultimate bearing capacity (in red), residual strength (in green) and structural stiffness (in orange).  $\square$ ,  $\circ$ ,  $\triangle$  representing data points from two-scale models;  $---$ ,  $---$ ,  $---$ , representing curves according to Eqs. (30)-(32), respectively. (a) Particle's radius is 5 mm; (b) particle's radius is 6 mm

are different.

From the above analyses, it is known that if the discrete particle assembly is large enough, the macro stiffness, the ultimate bearing capacity and the residual strength of the granular material structure tend to be the representative values. However, for a specified SDPA used in two-scale modeling, what are the predictions of the macro stiffness, the ultimate bearing capacity and the

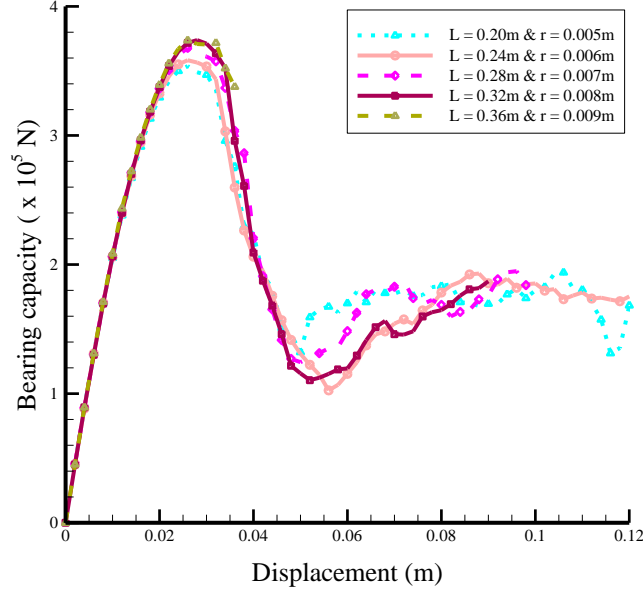


Fig. 6 Curves of vertical loading displacement vs. bearing capacity

residual strength? Or, if some values of the macro property and a response to the value of the SDPA are provided, how can the representative value and the size of RVE be obtained? To answer the above questions, three equations linking representative properties and SDPA sizes are suggested as follows using the fitting data in Fig. 3

$$\ln(F_u/F_u^{cr}) = a_u \cdot e^{b_u \cdot (V/V^{cr})^2} = a_u \cdot e^{b_u^* \cdot V^2}, \quad (30)$$

$$\ln(F_{res}/F_{res}^{cr}) = a_{res} \cdot e^{b_{res} \cdot (V/V^{cr})^3} = a_{res} \cdot e^{b_{res}^* \cdot V^3}, \quad (31)$$

$$\ln(E/E^{cr}) = a_E \cdot e^{b_E \cdot (V/V^{cr})} = a_E \cdot e^{b_E^* \cdot V}, \quad (32)$$

where  $V$  is the size of the current particle assembly (it stands area under 2D case),  $F_u$ ,  $F_{res}$  and  $E$  are, respectively, the ultimate bearing capacity, the residual strength and the macro structure stiffness responding to the current particle assembly.  $F_u^{cr}$ ,  $F_{res}^{cr}$ ,  $E^{cr}$  and  $V^{cr}$  are critical representative values of the ultimate bearing capacity, the residual strength, the macro stiffness and the size of RVE, respectively.  $a_i$ ,  $b_i$  ( $i=u, res, E$ ) are constant coefficient parameters. When  $V^{cr}$  is determined,  $b_i$  and  $V^{cr}$  can be combined as  $b_i^*$ , meaning each equation has only three independent variables. Based on the data from Fig. 4 and Eqs. (30)-(32), the fitting curves are shown in Fig. 5(a). It can be seen that the above equations, which obey the logarithmic-exponential law, agree well with those data points. It must be noted that different macro structure properties have different sensibilities on the SDPA. Fig. 5 shows that the prediction of residual strength is about 105% of the representing value when the current SDPA is about 75% of the critical RVE size, while the prediction of the macro stiffness is about 95% of the representing value when the current SDPA is about 60% of the critical RVE size. This indicates that the residual strength remains the most dependent on the SDPA, while the macro stiffness depends the least on it. In order to further verify

the universality of the logarithmic-exponential law, Fig. 5(b) shows the macro properties predicted by two-scale modeling in which the discrete particle assembly consists of 6mm round particles has been adopted at the micro level; it can be seen that the logarithmic-exponential curves match data points very well.

Chang (1990) suggested a relationship between the macro stiffness and micro stiffness at contact points based on a regular packing structure

$$\bar{E} = \frac{2r^2 N_c}{15V} (2k_n + 3k_s) \left( \frac{5k_n}{4k_n + k_s} \right) , \quad (33)$$

From Eq. (33), it can be seen that the macro stiffness is inversely proportional to the size ( $V$ ) of the particle assembly, however proportional to the particle's radius ( $r^2$ ). It has been noted that the symbol  $V$  represents the size of the discrete particle assembly. To compare the macro stiffness predicted using this two-scale scheme with the theoretical expression, Fig. 6 shows the curves of the bearing capacity vs. the vertical loading displacement under a fixed ratio ( $r^2/V=1600$ ) between the particle's radius and the size of the assembly. It can be seen that the corresponding macro stiffness of all samples are the same because  $N_c$  is almost constant in the elastic range. From Fig. 4, it can be seen that the macro stiffness increases with the corresponding sample's increasing size to approach a limit value for all the assemblies with the same radius particle. The reason for this is that the ratio between the total number of contacts  $N_c$  and the sample size  $V$  will remain constant when the sample size is big enough, consisting of the same radius particle. Based on the above comparison, a prediction regarding the influence of the assembly's size and the particle's radius on the macro stiffness are consistent with Chang's theoretical formula; this indicates to some extent the validity of the two-scale model program used in this paper.

It is noteworthy that Gitman *et al.* (2008) think there are no dependencies in the cases of linear-elasticity and hardening; however, there is a strong dependency on both the macro-level mesh size and the meso-level cell size in cases of softening. The dependency of a meso-level cell size indicates there is no RVE. Because softening is one of the essential behaviors of granular materials, it is necessary to check the existence of RVE for a two-scale computational scheme of granular materials. To this aim, we adopted the Cosserat continuum to avoid the macro-level mesh size (Muhlhaus and Vardoulakis 1987, Chang *et al.* 2014), and to investigate macro responses using varying sizes of discrete particle assemblies. Our simulation results showed there are links between different macro physical properties (responses) and the SDPA, viz. Eqs. (30)-(32). From these equations and Figs. 4 and 5, it can be seen that there are RVEs for granular materials. In fact, there are some works on two-scale models of granular materials (Christian and Peter 2012, Nitka *et al.* 2011, Guo and Zhao 2014); these two-scale models can predict the behavior of granular materials (including localization and softening) from the premise that the RVE exists for granular materials.

#### 4. Evolutions of the discrete particle assembly

In this section, we will investigate the configuration evolution and the displacement fluctuation of the discrete particle assembly on the micro scale based on two-scale models. On the macro level, a  $5 \times 5 \text{ m}^2$  homogeneous square panel was meshed into 100 elements and the vertical load was applied to the top and bottom of the square panel with prescribed increasing vertical displacement, as shown in Fig. 7(a). The discrete particle assembly consisted of 5 mm round

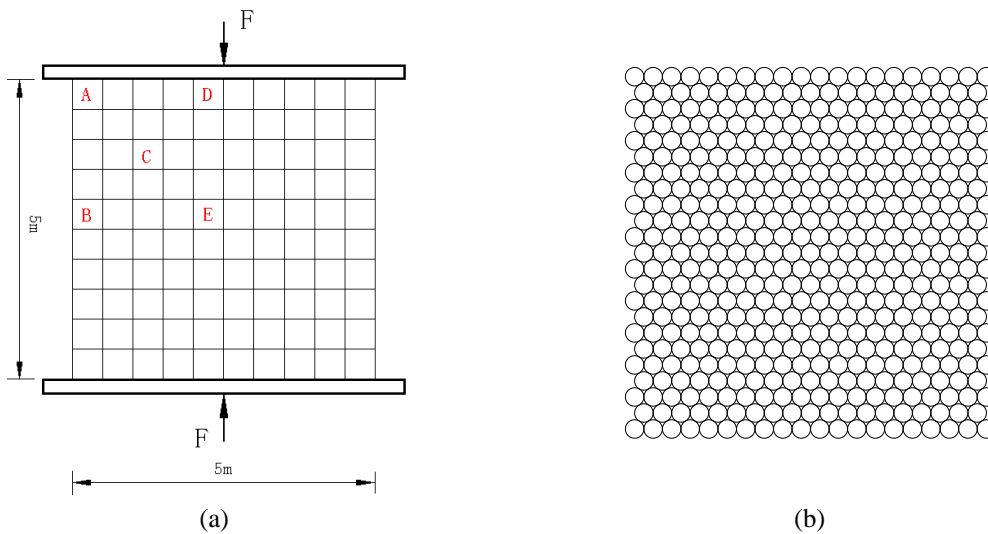


Fig. 7 Sketch of model 2: (a) FEM model; (b) The discrete particle assembly

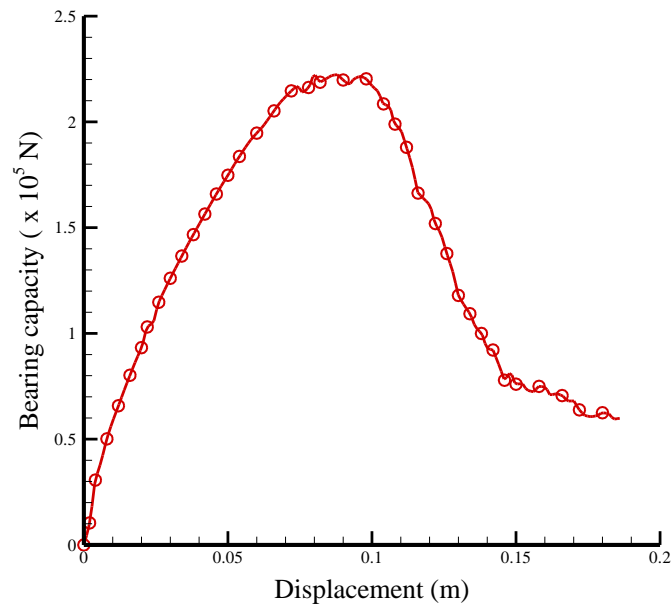


Fig. 8 Curve of vertical loading displacement vs. bearing capacity

particles with a dense arrangement form, as shown in Fig. 7(b). The micro parameter values used in the simulation are the same as those in the example shown in Section 3.

Fig. 8 shows the curve of bearing capacity vs. the vertical loading displacement. It can be seen that this curve has same tendency as the curve in Fig. 3. Fig. 9 shows the macro strain's distribution under different vertical load displacements. It can be seen there is significant macro strain localization in the panel at displacement 0.04 m before the bearing capacity (Fig. 9(a)). Here, the macro strain in Fig. 9 is an equivalent strain, which is calculated as



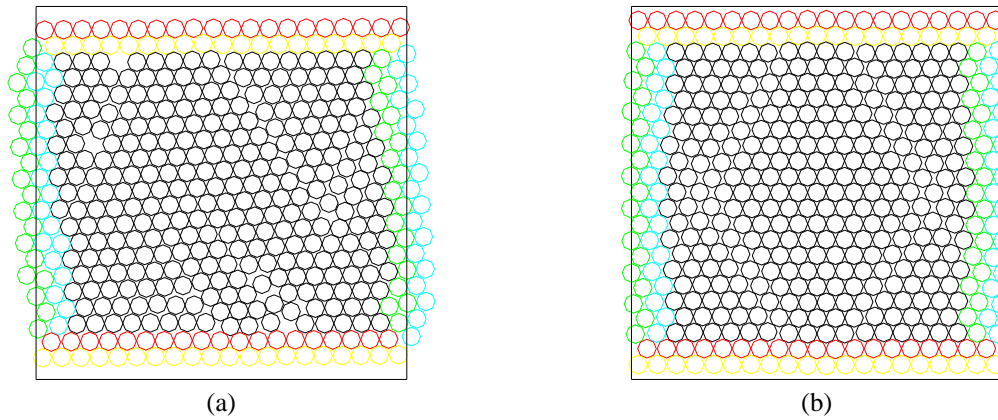


Fig. 10 The typical configuration of the assembly at different Gauss integral points when the vertical loading displacement is 0.08 m: (a) a Gauss integral point of Element A; (b) a Gauss integral point of Element E

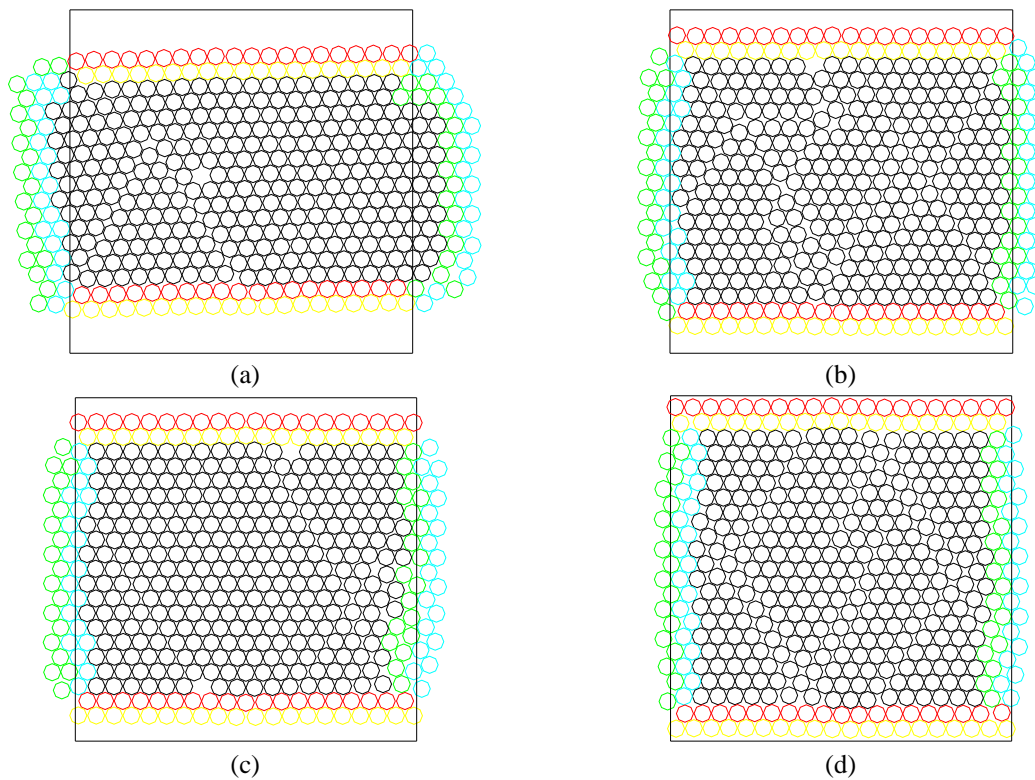


Fig. 11 The typical configuration of the assembly at different Gauss integral points when the vertical loading displacement is 0.18 m: (a) a Gauss integral point of Element A; (b) a Gauss integral point of Element E; (c) b Gauss integral point of Element D; (d) a Gauss integral point of Element B

theories have been successfully applied to overcome this problem (Muhlhaus and Vardoulakis 1987, Chang *et al.* 2014). Therefore, the macro-level mesh dependency has not been tested in this two-scale model of localization based on the discrete particle model on the micro level and the

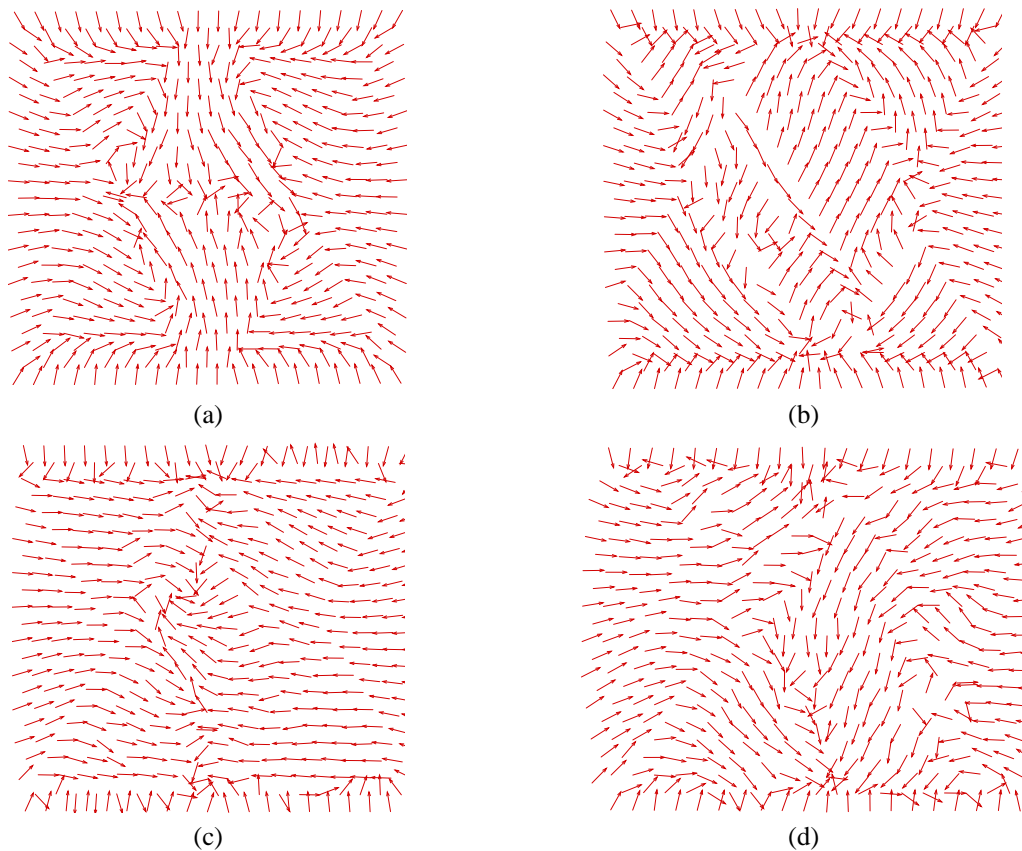


Fig. 12 The typical displacement fluctuation of the assembly at Element A under different vertical loading displacements: (a) 0.04 m; (b) 0.08 m; (c) 0.12 m; (d) 0.18 m

Cosserat continuum on the macro level.

The bearing capacity reached vertical displacement at 0.08 m (Fig. 8); at this point the strain localization (Fig. 9(b)) is less apparent than what is shown in Fig. 9(a). The strain localization will disappear at displacement 0.12 m and 0.18 m (Fig. 9(c) and 9(d)). To investigate the micro mechanism contribution to the above phenomena, we can see in Figs. 10 and 11 some typical configurations of the assembly at different integration points corresponding to the load displacements 0.08 m and 0.18 m, respectively. The black frame in Figs. 10 and 11 was used to compare changes in the configuration of the discrete particle assembly. As shown in Fig. 10(a), it is evident, given the assembly configuration at the integral point located at Element A, that the particles on the boundary present obvious movement; the closely packed form is also broken. This micro-phenomenon is consistent with the larger macro deformation at Element A. Meanwhile these assemblies have managed to remain close to their original configurations, as shown in Fig. 10(b) at other integration points where macro deformation is not obvious. When vertical displacement reaches 0.18 m, there are distinct forms in the rearrangements of particle assemblies at different locations. A few obvious voids appear in the particle assembly at Element A, as shown in Fig. 11(a), despite that the discrete particle assembly restored a closely packed form. Unlike the particle assembly at Element A, some obvious voids appeared in the assembly at Element E, as

shown in Fig. 11(b), and a portion of particles were less closely packed. Meanwhile, Fig. 11(c) shows there are few voids in the internal assembly at Element D, but the entire assembly maintained a complete closely packed form. The almost assemblies at other elements have some micro-slide band to some extent, as shown in Fig. 11(d). In addition, some reports have indicated that the strain localization of granular material is closely related to the non-affine deformation, and particle displacement fluctuations show a vortex form (Abedi *et al.* 2012). To investigate the evolution of particle displacement fluctuation with macro deformation, Fig. 12 shows the particle displacement fluctuations of the assembly at Element A's integral point. The residual displacement ( $u^R$ ) is defined as the difference between the real displacement ( $u$ ) and the affine displacement ( $u^a$ )

$$u_i^R = u_i - u_i^a = u_i - l_i \varepsilon_i, \quad (35)$$

where  $l_i$  is the branch vector,  $\varepsilon_i$  is the macro strain vector.

In Fig. 12, the particle displacement fluctuations are all unitized; the arrow lines in the Figure represent the direction of the particles' displacement fluctuation. During early loading particle displacement, the fluctuations show four symmetric slide bands (where the residual displacement goes in the opposite direction) with two axes of symmetry (Fig. 12(a)). When loading displacement reached 0.08 m (almost corresponding to the bear capacity), more slide bands appeared (Fig. 12(b)), indicating that particles have the severe non-uniform motion. However, at displacement 0.12 m, after the bear capacity, the number of slide bands reduced and the left and right parts of the particle displacement fluctuations in the panel were presented symmetrically (Fig. 12(c)). When corresponding to the residual stage (at displacement 0.18 m), the residual displacement was as complex as that shown in Fig. 12(b); however, the slide bands in the top and bottom portion of the panel are more obvious. Given the evolution of the residual displacement fields above, our work indicates there is a pattern that leads from orderliness to chaos and back to orderliness. Relating to macro deformation, this responds to the phenomena from the failure pattern of the regular shear band to the diffuse failure pattern.

## 5. Conclusions

Granular materials have obvious size effects. The discrete particle assembly used in two-scale models plays an important role regarding the prediction results of granular structures. This work focused largely on the size of the discrete particle assembly and the radius of the particle in the assembly and its influence on deformation stiffness, bearing capacity and the residual strength of a granular structure. According to the numerical results, we suggest corresponding fitting formulas linking the values of different macro physical properties with the size of discrete particle assemblies. The significance of these formulas is that they confirm the existence of RVE. More importantly, these formulas can predict the representing values of physical properties and the size of the corresponding RVE only requires a few values regarding relevant physical properties and the corresponding SDPA.

In addition, we were also concerned with the strain localization on the macro level and the configuration and displacement fluctuations of the assembly during the loading process. The Cosserat continuum was adopted to avoid the macro-level mesh size strain localization. We believed that the rotation and couple-stress would affect the RVE size; however, that matter was not a focus in this study. Numerical results showed that the macro deformation was closely associated with the evolution of the discrete particle assembly, although the closely packed form of

the discrete particle assembly did not undergo any obvious changes before the ultimate bearing capacity. However, the non-affine displacement of the particle assembly will be dominant when approaching the ultimate bearing capacity. After the ultimate bearing capacity, the closely packed form of the assembly gradually disappeared; as a result, the bearing capacity softened significantly. Other interesting phenomena occurred between the ultimate bearing capacity to the residual stage. The number of slip bands in the displacement fluctuation field reduced and symmetry reappeared; a disorder distribution of residual displacement was present at the residual stage.

## Acknowledgements

The authors are pleased to acknowledge the support of this work by the National Natural Science Foundation of China through contract/grant number 11472196 and 11172216, and the Natural Key Basic Research and Development Program of China (973 Program) through contract/grant numbers 2010CB731502. The authors also thank the reviewers for their constructive comments and suggestions.

## Reference

- Abedi, S., Rechenmacher A.L. and Orlando, A.D. (2012), "Vortex formation and dissolution in sheared sands", *Granular Matter.*, **14**, 695-705.
- Chang, C.S. and Misra, A. (1990), "Packing structure and mechanical properties of granulates", *J. Eng. Mech.*, **116**(5), 1077-1093.
- Cil, M.B. and Alshibli, K.A. (2014), "3D analysis of kinematic behavior of granular materials in triaxial testing using DEM with flexible membrane boundary", *Acta Geotechnica*, **9**(2), 287-298.
- Chang, J.F., Chu, X.H. and Xu, Y.J. (2014), "Finite Element Analysis of failure in transversely isotropic geomaterials", *Int. J. Geomech.*, 10.1061/(ASCE)GM.1943-5622.0000455, 04014096.
- Christian, W. and Peter, W. (2012), "A two-scale model of granular materials", *Comput. Meth. Appl. Mech. Eng.*, **205**, 46-58.
- Gitman, I.M., Askes, H. and Sluys, L.J. (2007), "Representative volume: Existence and size determination", *Eng. Fract. Mech.*, **74**(16), 2518-2534.
- Graham, S. and Yang, N. (2003), "Representative volumes of materials based on microstructural statistics", *Scripta Materialia*, **48**, 269-274.
- Gitman, I.M., Askes, H. and Sluys, L.J. (2008), "Coupled-Volume multi-scale modeling of quasi-brittle material", *Eur. J. Mech. A Solid.*, **27**, 302-327.
- Guo, N. and Zhao, J.D. (2014), "A coupled FEM/DEM approach for hierarchical multiscale modeling of granular media", *Int. J. Numer. Meth. Eng.*, **99**, 789-818.
- Hill, R. (1985), "On the micro-to-macro transition in constitutive analyses of elastoplastic response at finite strain", *Math. Pr. Cambrid. Phil. Soc.*, **98**, 578-590.
- Huang, X., Hanley, K.J., Sullivan, O. *et al.* (2014), "Effect of sample size on the response of DEM samples with a realistic grading", *Particuol.*, **15**, 107-115.
- Jiang, M.J., Li, T., Hu, H.J. and Thornton, C. (2014), "DEM analyses of one-dimensional compression and collapse behaviour of unsaturated structural loess", *Comput. Geotech.*, **60**, 47-60.
- Koyama, T. and Jing, L. (2007), "Effects of model scale and particle size on micro-mechanical properties and failure processes of rocks-a particle mechanics approach", *Eng. Anal. Bound. Elem.*, **31**, 458-472.
- Kuhn, M.R. and Bagi, K. (2009), "Specimen size effect in discrete element simulation granular assemblies", *J. Eng. Mech.*, **135**, 485-491.
- Li, X.K., Liu, Q.P. and Zhang, J.B. (2010), "A micro-macro homogenization approach for discrete particle

- assembly Cosserat continuum modeling of granular materials”, *Int. J. Solid. Struct.*, **47**, 291-303.
- Liu, Q.P., Liu, X.Y., Li, X.K. and Li, S.H. (2014), “Micro-macro homogenization of granular materials based on the average-field theory of Cosserat continuum”, *Adv. Powder Tech.*, **25**, 436-449.
- Miehe, C., Dettmar, J. and Zah, D. (2010), “Homogenization and two-scale simulations of granular materials for different microstructural constraints”, *Int. J. Numer. Meth. Eng.*, **83**, 1206-1236.
- Muhlhaus, H.B. and Vardoulakis, I. (1987), “The thickness of shear bands in granular materials”, *Geotechniq.*, **37**, 271-283.
- Nitka, M., Combe, G., Dascalu, C. *et al.* (2011), “Two-scale modeling of granular materials: a dem-fem approach”, *Granular Matter*, **13**, 277-281.
- Scholtes, L. and Donze, F.V. (2013), “A DEM model for soft and hard rocks: Role of grain interlocking on strength”, *J. Mech. Phys. Solid.*, **61**(2), 352-369.
- Shen, H. (2001), “Sample size effects on constitutive relations of granular materials- a numerical simulation study with two-dimensional flow of disks”, *J. Eng. Mech.*, **127**, 978-986.
- Voyiadjis, G.Z., Alsaleh, M.I. and Alshibli, K.A. (2005), “Evolving internal length scales in plastic strain localization for granular materials”, *Int. J. Plast.*, **21**, 2000-2024.
- Wan, K. and Li, X.K. (2013), “Bridging scale method for Biot-Cosserat continuum-discrete particle assembly modeling of unsaturated soil”, *Chin. J. Appl. Mech.*, **30**(3), 297-304. (in Chinese)
- Yu, C., Chu, X.H., Tang, H.X. and Xu, Y.J. (2013), “Study of effect of particle breakage based on Cosserat continuum”, *Rock Soil Mech.*, **34**(supp1), 67-73. (in Chinese)
- Zhou, G.D. and Sun, Q.C. (2013), “Three-dimensional numerical study on flow regimes of dry granular flows by DEM”, *Powder Technol.*, **239**, 115-127.
- Zhao, Y.H., Chang, J.M. and Gao, H.B. (2015), “On geometry dependent R-curve from size effect law for concrete-like quasibrittle materials”, *Comput. Concrete*, **15**(4), 673-686.